Macromolecules

ARTICLE

pubs.acs.org/Macromolecules

Flexible Solid Polymer Electrolytes Based on Nitrile Butadiene Rubber/Poly(ethylene oxide) Interpenetrating Polymer Networks Containing Either LiTFSI or EMITFSI

Laurent J. Goujon, Alexandre Khaldi, Ali Maziz, Cédric Plesse, Giao T. M. Nguyen, Pierre-Henri Aubert, Frédéric Vidal,* Claude Chevrot, and Dominique Teyssié

Laboratoire de Physicochimie des Polymères et des Interfaces (EA 2528), Institut des Matériaux (FD 4122), Université de Cergy-Pontoise, 5 mail Gay-Lussac, 95031 Cergy-Pontoise Cedex, France

ABSTRACT: The synthesis and characterization of flexible solid polymer electrolytes (SPEs) based on interpenetrating polymer networks (IPNs) are discussed. IPNs were prepared from nitrile butadiene rubber (NBR) and poly(ethylene oxide) (PEO) using a two-step process. The NBR network was obtained by dicumyl peroxide cross-linking at high temperature and pressure. A free radical copolymerization of poly(ethylene glycol) methacrylate and dimethacrylate led to the formation of the PEO network within the NBR network. Polymerization kinetics were followed by dynamic mechanical analysis (DMA) for the NBR network and by Fourier transform spectroscopy in the near- and mid-infrared for the PEO network. IPN mechanical properties, examined using DMA and tensile strength tests, reveal an IPN elongation with a breaking point of 110%. IPN conductivities reach 7.4×10^{-7} S cm^{-1} at 30 °C when doped with lithium bis(trifluoromethanesulfonyl)imide (LiTFSI). Moreover, IPNs exhibit an ionic conductivity as high as 0.7×10^{-3} S cm^{-1} at 30 °C when swollen in *N*-ethylmethylimidazolium bis(trifluoromethanesulfonyl)imide ionic liquid (EMITFSI).

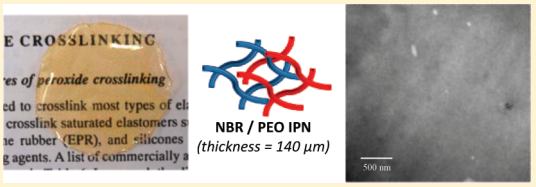

1. INTRODUCTION

Since Wright's discovery of ionic conduction in polymers containing inorganic salts[1] and Armand's discovery of the potential use of polymer ionic conductors as electrolytes,[2] a wide range of solid polymer electrolytes (SPEs)[3,4] have been developed in various electrochemical devices such as rechargeable batteries, sensors, actuators, electrochromic devices, and supercapacitors. Polyethers, typically poly(ethylene oxide) (PEO),[3−6] can be used as SPEs after complexation with various lithium salts. Nevertheless, PEO tends to present a high degree of crystallinity which decreases the specific conductivity, typically 10^{-5} S cm^{-1} at 25 °C in the presence of LiTFSI.[7] The formation of gel-like films, i.e., polymers swollen with an electrolytic solution, increases the specific conductivity[8] to a value as high as 1.5×10^{-3} S cm^{-1} at 30 °C.[9] However, gel-like films become sticky and lose their mechanical properties due to the large amount of electrolytic solution absorbed. Depending on their type, highly swollen polymer gels often do not have the ability to hold their shape when subjected to even small load levels.

In order to improve SPE mechanical properties, several elastomers such as natural rubber (NR), nitrile butadiene rubber (NBR), or styrene butadiene rubber (SBR) mixed with lithium salts or ionic liquids were studied,[10−12] but their poor dimensional stability remains a drawback. In order to solve the dimensional stability issue, SPEs can be designed as networks. In spite of improved mechanical properties and better dimensional stability, reducing the mobility of polymer chains decreases the material's charge mobility and, therefore, leads to a drop in ionic conductivity.[11,13] To overcome this problem, dangling chains can be introduced since this increases the proportion of free volume available for the migration of ions.[14−17] Similarly, a cross-linking agent containing a flexible spacer[13] can also be used to prevent a sharp decrease in ionic conductivity. Nevertheless, in all cases, it remains difficult to combine high ionic conductivity with good mechanical properties.[18] The properties of SPE materials have, therefore, been tailored and improved by using a physical or chemical combination of two or more structurally different polymers. Efforts to reduce crystallinity using blends[19−21] induces the problem of phase separation in such systems. Among the various structural modifications such as copolymerization,[22,23] grafting,[24] and cross-linking,[18,25−29] the formation of polymer networks has been suggested to be the most effective strategy to achieve low levels of crystallinity as well as good dimensional stability. For this purpose, interpenetrating polymer networks (IPNs) are a special class of networks which can be designed to fulfill specific end uses. IPNs are described as an intimate combination of two (or more) cross-linked polymers.[30] The tight entanglement of these networks ensures good interpenetration of the two components, and the 3-dimensional interpenetration in the networks radically improves dimensional stability. It also reduces the crystallinity and phase separation. In addition, an improved combination of the component's various properties can also sometimes be attained.

Therefore, in order to obtain a soft, flexible, and self-supporting SPE designed as starting materials in actuators and electrochromic field, IPN architectures have been chosen since they

Received: July 20, 2011
Revised: October 20, 2011
Published: November 21, 2011

combine high ionic conductivity, good mechanical properties, and dimensional stability. This work presents NBR/PEO IPN synthesis using a two-step process with various IPN compositions. IPN syntheses and mechanical properties, especially viscoelasticity, dimensional stability, and tensile strength, have been analyzed. Second, the ionic conductivity properties of NBR/PEO IPNs were studied using LiTFSI and EMITFSI (an ionic liquid) as electrolyte. The thorough study on IPNs ionic conductivity in the presence of Li salt enables to understand the morphology and to confirm the cocontinuous architecture of IPN. Lastly, by using EMITFSI as electrolyte in a material with known morphology, high ionic conductivity could be obtained. The influence of temperature and electrolyte contents on ionic conductivity of the membrane is presented as well as the relationship between mechanical properties and electrolyte contents.

2. EXPERIMENTAL SECTION

2.1. Chemicals. Nitrile butadiene rubber with 44 wt % acrylonitrile content (NBR, M_w = 230 000 g mol^{-1}, Perbunan 4456F Lanxess), dicumyl peroxide (DCP, Aldrich, 98%), poly(ethylene glycol) dimethacrylate (PEGDM, M_n = 750 g mol^{-1}, Aldrich), poly(ethylene glycol) methyl ether methacrylate (PEGM, M_n = 475 g mol^{-1}, Aldrich), and hydroquinone (Aldrich, 99%) were used without further purification. Cyclohexanone (Acros, 99.8%), dichloromethane (VWR, grade 99%), propylene carbonate (Acros, 99.5%), bis(trifluoromethane)sulfonamide lithium salt (LiTFSI, Aldrich), and *N*-ethylmethylimidazolium bis(trifluoromethane)imide (EMITFSI, Solvionic, electrochemical grade 99%) were used as received. 2,2′-Azobis(isobutyronitrile) (AIBN) (Aldrich) was recrystallized from methanol before use.

2.2. Synthesis. *2.2.1. Preparation of Single Networks.* NBR single networks were prepared through the following procedure: 48 g of NBR was introduced in the mixing chamber of a Haake PolyLab OS with roller-rotors speed of 50 rpm at 100 °C for 10 min. 0.96 g of DCP was added, and the blend was mixed for an additional 10 min. The prepared blend was further molded under pressure and cross-linked in a hydraulic-heated press at 180 °C and a pressure of 285 kg cm^{-2} for 30 min. Finally, NBR films were removed from the mold, washed by dichloromethane in Soxhlet for 1 week to extract chemical additives, and dried at 50 °C under vacuum. The extractible content is close to 4%. NBR single networks are 110 μm thick.

PEO single networks were prepared according to a described procedure.[31] Typically, PEGM and PEGDM were magnetically stirred together in a flask under vacuum for 45 min at room temperature. AIBN (3 wt % with respect to the total weight of methacrylate monomers) was introduced, and the mixture was stirred for an additional 30 min under vacuum. The mixture was then poured into a mold made from two glass plates clamped together and sealed with a 500 μm thick Teflon gasket. The mold was then kept at 70 °C for 1 h. The sample was postcured 1 h at 100 °C.

A series of PEO networks were prepared with different PEGM/PEGDM ratios: (25/75), (50/50), and (75/25), further named PEO(75% PEGDM), PEO(50% PEGDM), and PEO(25% PEGDM), respectively.

2.2.2. Preparation of IPNs. NBR/PEO IPNs were prepared through a two-step process (Figure 1): PEGM, PEGDM, and cyclohexanone (ratio between PEO precursors and cyclohexanone = 75/25 by weight) were stirred together under vacuum for 45 min at room temperature. AIBN (3 wt % with respect to the total weight of methacrylate oligomers) was introduced, and the mixture was stirred an additional 30 min under vacuum. The aimed NBR/PEO ratio in the final material is about 50/50 wt/wt. NBR single network films, previously prepared and

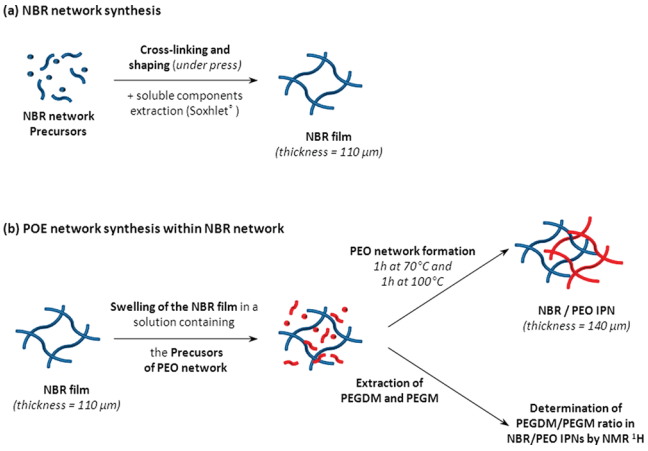

Figure 1. Outline of NBR/PEO IPN synthesis.

washed, were swollen in the cyclohexanone solution of PEO precursors for 3 h, wiped carefully with filter paper, and positioned between two glass plates. Samples were kept 1 h at 70 °C and 1 h at 100 °C. Resulting NBR/PEO IPNs were then dried 24 h at 70 °C under vacuum. Free-standing NBR/PEO IPNs are thus obtained with a thickness of 140 μm. Three solutions of PEO precursors and cyclohexanone were prepared with different PEGM/PEGDM ratios: (25/75), (50/50), and (75/25). The three NBR/PEO IPNs obtained were named NBR/PEO(75% PEGDM), NBR/PEO(50% PEGDM), and NBR/PEO(25% PEGDM), respectively.

2.2.3. Determination of PEGDM/PEGM Ratio in NBR/PEO IPNs. NBR single network films were swollen in the cyclohexanone solutions of PEO precursors for 3 h without AIBN. The introduced PEGDM and PEGM were extracted by washing the film with dichloromethane five times (Figure 1). The PEGDM/PEGM ratio was determined by ^{1}H NMR using a calibration curve. This calibration curve was established by ^{1}H NMR (Bruker ADVANCE-DPX250). The ratio of PEGM/PEGDM incorporated in the NBR network is calculated from the following integrations at 3.2 ppm corresponding to the O−CH_3 signal of PEGM and at 6.0 and 5.4 ppm corresponding to the =CH_2 signals of PEGM and PEGDM.

2.3. Kinetic Experiments. Dynamic mechanical analysis (DMA) measurement allows studying NBR cross-linking kinetics by following the storage modulus of NBR as a function of time. Experiments were performed with a Q800 model (TA Instruments) at 1 Hz frequency, operating in tension mode (strain: 0.07%; pretension: 10^{-2} N) on samples of 7 mm long, 6 mm width, and 2 mm thick. Different cross-linking temperatures were studied (160, 180, and 200 °C).

The PEO cross-linking kinetics inside the NBR single network was monitored using the previously described procedure:[32] NBR films (2 mm thickness), swollen by a cyclohexanone solution of PEO precursors, were directly introduced between two glass plates of an IR cell. The IR cell was inserted into an electrical heating jacket with an automatic temperature controller (Graseby Specac) and the block temperature being constant within ±1 °C of the set temperature. The infrared and near-infrared spectra were recorded with a Fourier transform infrared spectrometer (Bruker Equinox 55) in the 4000−7000 cm^{-1} range by averaging 16 consecutive scans with a resolution of 4 cm^{-1}. The methacrylate group conversion versus time was observed at the corresponding harmonic absorption band located in the near-infrared (6160 cm^{-1}).

2.4. Characterization of Single Networks and IPN. *2.4.1. Soxhlet Extraction.* In order to estimate the amount of unreacted starting material in the final product (single network, IPN) and thus

the efficiency of cross-linking reactions, a known weight of the product was extracted in a Soxhlet with dichloromethane for 1 week. After extraction the sample was dried in a vacuum oven for 8 h at 30 °C. The extractible content (EC) is given as a weight percentage:

$$\mathrm{EC}\ (\%) = \frac{W_0 - W_e}{W_0} \times 100 \quad (1)$$

where W_0 and W_e are the sample weights before and after extraction, respectively.

2.4.2. Dynamic Mechanical Analysis (DMA). Dynamic mechanical analysis measurements were carried out on samples (typically $L \times w \times t = 6 \times 9 \times 0.11$ (mm) for NBR single networks; $L \times w \times t = 10 \times 8 \times 0.5$ (mm) for PEO single networks; $L \times w \times t = 6 \times 8 \times 0.14$ (mm) for IPNs) operating in tension mode (strain: 0.07%; pretension: 10^{-2} N). Experiments were performed at 1 Hz frequency and with a heating rate of 3 °C min^{-1} from −80 to 100 °C. The setup provided the storage and loss moduli (E' and E''), and the damping parameter or loss factor (tan δ) was defined as tan $\delta = E''/E'$.

2.4.3. Transmission Electron Microscopy (TEM). TEM analysis was performed by the Centre de Microscopie Electronique Stéphanois (St Etienne, France) with a Hitachi H-800 microscope. The samples were previously cut by cryo-ultramicrotomy and then exposed to osmium tetraoxide steam for 20 min.

2.4.4. Mechanical Properties. Creep tests were carried out on a NBR/PEO(50%PEGDM) IPN (typically $L \times w \times t = 6 \times 9 \times 0.14$ (mm)) by DMA operating in tension mode (pretension: 10^{-2} N) at 25 °C. The sample strain as a function of time was studied for different stress levels for 10 min and for a recovery time of 10 min. The strain recovery (S_r) is calculated using the equation

$$S_r = \frac{S - S_f}{S} \times 100 \quad (2)$$

where S is the sample strain after 10 min under stress and S_f the sample strain after 10 min of recovery time.

Mechanical elongations were measured by a mechanical testing machine (UNIMAT plus 050-2kN (ERICHSEN) interfaced with a computer. Samples were cut in strips (typically $L \times w \times t = 10 \times 10 \times 0.11$ (mm) for NBR single networks; $L \times w \times t = 10 \times 10 \times 0.5$ (mm) for PEO single networks; $L \times w \times t = 10 \times 10 \times 0.14$ (mm) for IPN samples). The strips were fixed between two clamps, drawn by a constant velocity (20 cm min^{-1}) at room temperature, and the stress as a function of the strain was recorded.

2.4.5. Thermal Analysis. Differential scanning calorimetry (DSC) measurements were carried out in the temperature range −90 to 220 °C in a Q100 model (TA Instruments) with a heating rate of 10 °C min^{-1} under an argon atmosphere. Thermogravimetric analysis (TGA) was performed under synthetic air (79.5% N_2, 20.5% O_2) on a Q50 model (TA Instruments) applying a heating rate of 20 °C min^{-1} from room temperature to 800 °C.

2.4.6. Ionic Conductivity. The ionic conductivity was determined by electrochemical impedance spectroscopy with a VSP potentiostat (Biologic SA). The films were sandwiched between two stainless steel electrodes and placed in a thermostat cell under an argon atmosphere. Experiments were carried out in a temperature range from 20 to 100 °C by steps of 5 °C, in the frequency range from 1 MHz to 0.01 Hz with a rate of 6 points per decades and for an oscillation potential of 10 mV. The ionic conductivity (S cm^{-1}) is calculated using the equation

$$\sigma = \frac{1}{Z}\frac{d}{S} \quad (3)$$

where Z is the real part of the complex impedance (ohms), d the thickness of the sample, and S is the sample area (cm^2).

2.4.7. Swelling Degree (SD) and $[Li^+]/[-CH_2-CH_2-O-]$ Ratio. The swelling degree in the samples was defined as

$$\mathrm{SD} = \frac{W_S - W_0}{W_0} \times 100 \quad (4)$$

where W_0 and W_S are the weight of a polymer sample before and after swelling.

The molar ratio $[Li^+]/[-CH_2-CH_2-O-]$ is calculated according to the following calculations:

$$\frac{[Li^+]}{[CH_2 - CH_2 - O -]} = \frac{m_f - m_i}{M_{n,LiTFSI}} \frac{1}{x\left((1-y) \times \frac{9m_i}{M_{n,PEGM}}\right) + \left(y \times \frac{13.5m_i}{M_{n,PEGDM}}\right)} \quad (5)$$

where $[Li^+]$ is the mole number of LiTFSI loaded in the sample and $[-CH_2-CH_2-O]$ is the mole number of ethylene oxy units in the PEO network or in the PEO/NBR IPN. m_i and m_f are the sample weight before and after LiTFSI loading. $M_{n,LiTFSI}$, $M_{n,PEGM}$, and $M_{n,PEGDM}$ are molar weights of LiTFSI, PEGM, and PEGDM. x is the PEO network ratio in the sample. y is the PEGDM/PEGM ratio according to PEO network compositions.

3. RESULTS AND DISCUSSION

3.1. Single Networks and IPN Synthesis. The NBR single network is obtained by cross-linking in the presence of DCP (2 wt %) at high temperature and pressure. The advantage of using DCP is that the resulting network contains only relatively stable carbon−carbon bonds as junction units between chains. As a result, DCP cross-linking provides a higher thermal stability and a superior heat-aging resistance than does sulfur vulcanization which consists of $-C-S_x-C-$ units which can undergo structural rearrangement reactions.[33] After the cross-linking reaction, all the soluble components were eliminated from the NBR films by means of a Soxhlet extraction before characterization. Extractible contents were lower than 4%, indicating substantially the complete cross-linking of NBR. PEO single networks are synthesized by free-radical copolymerization of PEGM and PEGDM in the presence of AIBN (3 wt % with respect to PEGM and PEGDM). Their extractible contents were lower than 3%. Three PEO single networks were prepared with 25, 50, and 75 wt % PEGDM (referred to hereafter as PEO(25% PEGDM), PEO(50% PEGDM), and PEO(75% PEGDM), respectively).

A series of IPNs were synthesized using a sequential process in which the PEO network becomes interpenetrated in the NBR network (Figure 1). At first, the NBR networks were swollen with a solution containing PEGM, PEGDM, and AIBN in cyclohexanone. Three different PEGM/PEGDM weight ratios (25/75), (50/50), and (75/25) with constant concentration were studied (ratio between PEO precursors and cyclohexanone of 75/25 by weight). The formation of a PEO secondary network was then obtained using the same curing conditions as that used for the PEO single network. It was noticed that the increase in PEGDM cross-linker reduces the extractible content (Table 1). In all cases, NBR/PEO IPNs have extractible contents of less than 7 wt %, indicating that the PEO network was satisfactorily formed.

The content of PEO material in the IPN was determined by weighing the NBR sample during the IPN formation process

Table 1. IPNs Compositions and Extractible Contents as a Function of PEGDM/PEGM Initial Solutions

		NBR/PEO ratio		
PEGDM/PEGM ratio (w/w) in the cyclohexanone solution	PEGDM/PEGM ratio (w/w) in the swollen NBR network	by weighing	elementary analysis	extractible content (wt %)
25/75	35/65	51/49	52/48	7
50/50	52/48	54/46	55/45	5
75/25	75/25	57/43	58/42	4

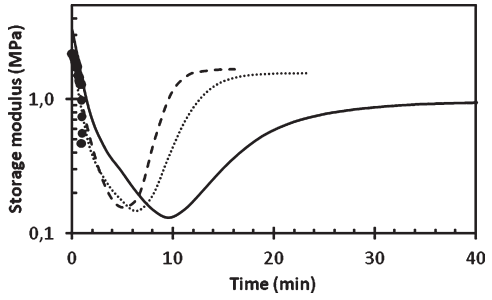

Figure 2. NBR storage modulus versus time: NBR network formation kinetic studies at 200 °C (dashed line), 180 °C (pointed line), and 160 °C (solid line) with 2% DCP and at 180 °C without DCP (●).

before the swelling step and after the drying step. Furthermore, the NBR/PEO ratios in the IPN were confirmed by elementary analysis. In addition, the composition of the PEO network was estimated by analyzing the precursor composition trapped within the NBR network immediately after the swelling step. For this purpose, the trapped precursors were extracted from the NBR network, and their composition was determined by ^{1}H NMR analysis.

The results are reported in Table 1. It can be seen that the content of PEGDM and PEGM oligomers in the NBR network are slightly different depending on the PEGM/PEGDM ratio. PEGDM seems to have more affinity to NBR than does PEGM. Swelling in a low PEGDM proportion solution, the swollen network is richer in PEGDM. The PEGDM proportion in the swollen network was found to be 35 wt % as opposed to the 25 wt % in solution. As the PEGDM ratio increases in the solution from 50 to 75 wt %, the composition in swollen NBR networks approaches the initial composition of the solution. On the other hand, the PEO ratio within the IPN decreases from 49 to 43 wt % as the PEGDM ratio increases from 35 to 75 wt %. These results can be used to obtain a precise composition of NBR/PEO IPNs.

3.2. IPN Formation Kinetic Studies. For the formation of NBR single networks, cross-linking reaction kinetics have been studied at three different temperatures (160, 180, and 200 °C) by observing the storage modulus change versus time using dynamic mechanical analysis (DMA) in tension mode (Figure 2). With 2% DCP, three steps were observed during the kinetic experiments. First, the storage modulus decreased due to the polymer chain flowing under high temperature and tensile stress. In a second step, an increase in the storage modulus reveals NBR flow compensation via the cross-linking reaction. Next, the storage modulus reaches a plateau value in the third step when NBR cross-linking is complete. The cross-linking time was defined as

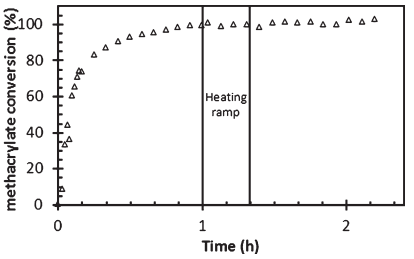

Figure 3. PEGDM/PEGM methacrylate conversion versus time for PEO(50% PEGDM) network formation within NBR network (FTIR overtone signal at 6160 cm^{-1}). The temperature is raised for 1 h at 100 °C after a 1 h curing at 70 °C (the transition time between the two temperatures is set at 20 min).

Table 2. T_α (°C), Strain (MPa), and Stress at Break (MPa) of Studied Networks and IPNs

networks	T_α (°C)	second relaxation	strain at break (%)	stress at break (MPa)
PEO 25% PEGDM	−40		<10	0.3
PEO 50% PEGDM	−32		<10	0.5
PEO 75% PEGDM	−29		<10	1.4
NBR	5		340	2.2
IPN 25% PEGDM	−2	−36 °C (shoulder)	110	1
IPN 50% PEGDM	2	−32 °C (shoulder)	110	1.2
IPN 75% PEGDM	4	−25 °C (shoulder)	110	1.7

the time it takes until the storage modulus reaches a plateau. Without DCP, the increase in the storage modulus is never observed because of the absence of a cross-linking reaction: after 1 min at 180 °C, the maximum clamp distance is attained.

By decreasing the temperature, the cross-linking time of the NBR single network increases, i.e., 15 min at 200 °C and 20 min at 180 °C (Figure 2). At 160 °C, even though the NBR storage modulus is still slowly increasing after 30 min, this indicates that the reaction is still ongoing.[34]

Second, the PEO network is formed within the NBR network. The PEO-swollen NBR films are cured for 1 h at 70 °C and postcured for 1 h at 100 °C. The radical copolymerization of methacrylate oligomers (PEGM and PEGDM), leading to the PEO network formation, takes place within the NBR network to form an interpenetrating polymer network. This second reaction is followed by FTIR spectroscopy in the near-infrared region using the $\nu_{CH_2=C(CH_3)-}$ overtone peak at 6160 cm^{-1}. After 1 h at 70 °C, the conversion is close to 100% (Figure 3).

3.3. IPN Dynamic Mechanical Analysis (DMA). The typical viscoelastic behavior of single networks was studied by DMA, and the results are reported in Table 2. Figure 4 depicts the loss factors (tan δ) of the NBR and three PEO single networks. For the NBR single network, the α relaxation temperature (T_α) is 5 °C. PEO single networks present a lower T_α than the NBR one. As expected, T_α values increase with the PEGDM content because the increase of the cross-linking density decreases the chain mobility in the PEO single network. T_α values are −40, −32, and −29 °C for PEO single networks with 25%, 50%, and 75% PEGDM, respectively.

In the case of IPNs (Figure 5), the α-relaxations observed at −2 to 4 °C correspond to the relaxation of NBR component in

dx.doi.org/10.1021/ma201662h |*Macromolecules* 2011, 44, 9683–9691

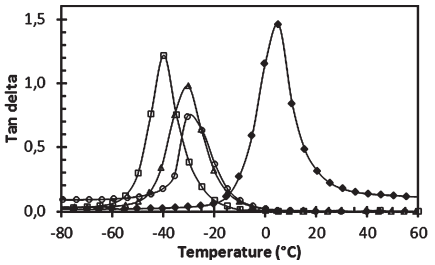

Figure 4. Dynamic mechanical analysis. Tan δ as a function of the temperature for NBR (◆) and PEO single networks (with 25% PEGDM (□), 50% PEGDM (△), and 75% PEGDM (○)).

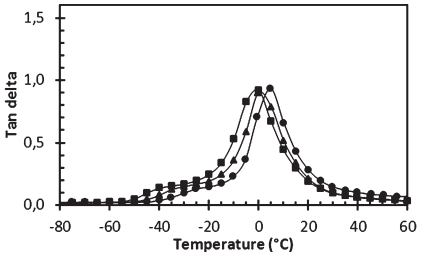

Figure 5. Dynamic mechanical analysis. Tan δ as a function of the temperature for NBR/PEO IPNs with 25% PEGDM (■), 50% PEGDM (▲), and 75% PEGDM (●).

the IPN. The T_α drop from 4 to −2 °C could be explained by a plasticization effect of the PEO chains to the segmental mobility of the NBR chains. A second α-relaxation was also observed in the form of a small shoulder at −36, −32, and −25 °C in the case of IPN with 25%, 50%, and 75% PEGDM, respectively. This relaxation could be related to the response of PEO partner within the IPN. This relaxation is shifted to higher temperature, compared with PEO single networks, due to the interpenetration of the PEO partner within the NBR network. The weakening and shifting PEO signal intensities in the IPNs leads to the conclusion that the IPN mechanical properties are mainly ruled by the NBR network. This result was expected since the NBR behaves as a continuous phase due to the synthetic pathway.

3.4. Microscopic Investigation. Transmission electron microscopy (TEM) observations were made on NBR/PEO samples stained with OsO_4. Figure 6a,b shows the TEM pictures of the NBR/PEO(50%PEGDM) IPN. Since only the butadiene segments of the NBR polymer can be marked with OsO_4, the black regions can be interpreted as being NBR-rich phases and PEO-rich phases appear as clear-gray regions. Since the TEM pictures are grayish, the boundaries between the dark and clear-gray regions is not obvious. This reinforces the fact that the IPN architecture is a very finely distributed PEO phase in a continuous NBR matrix. The PEO regions are less than 30 nm (see Figure 6b), which is consistent with the transparency of the sample. Nevertheless, some white areas, of a few hundred nanometers in width, appear on the picture and represent the PEO phases. The other IPN compositions (25% PEGDM and 75% PEGDM) have also been investigated by TEM and reveal similar morphologies.

3.5. IPN Mechanical Property Studies and Thermogravimetric Analysis. The mechanical properties were mainly studied using the sample containing an intermediate proportion of PEGDM. Creep tests were performed on NBR/PEO(50% PEGDM) IPN using DMA for various stress levels, i.e., 0.22, 0.35, and 0.45 MPa. Figure 7 depicts an IPN strain change during a 10 min stress time with a 10 min recovery time . The sample exhibited mainly elastic behavior with almost no chain creep. Whatever the applied stress, the strain recovery was always greater than 98%, which indicates that the IPN has good dimensional stability.

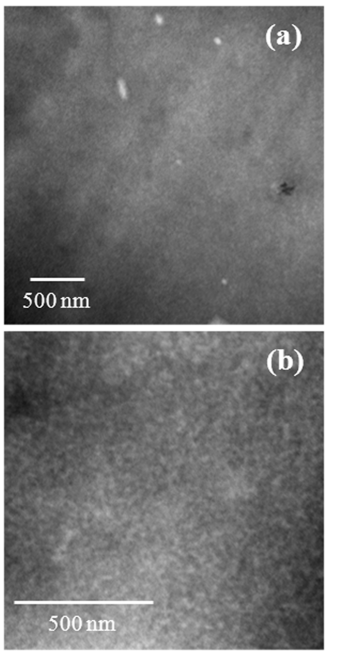

Figure 6. TEM pictures of NBR/PEO(50% PEGDM) IPN. Black domains can correspond to NBR-rich phases and white domains as PEO-rich phases.

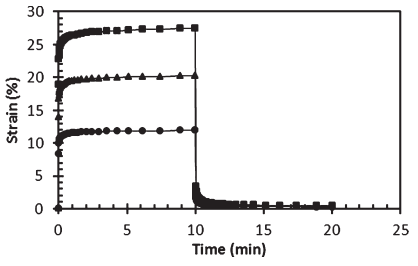

Figure 7. Variation of strain versus time for NBR/PEO(50% PEGDM) under three stress levels (0.22 MPa (●), 0.35 MPa (▲), and 0.45 MPa (■)) during 10 min and strain recovery of 10 min.

Tensile strength experiments (Figure 8a,b) show PEO single networks have minimal elongation with a break lower than 10% strain. On the other hand, NBR single network breaks at 340% strain. IPNs exhibit an intermediate behavior between those of the two partner networks. The elongation at break is close to 110% regardless of the PEGDM content. Nevertheless, the relationship between the stress at break of the PEO networks and IPNs with various PEGDM cross-linker compositions was observed. The stress at break increases with increasing PEO cross-linking content. The values of stresses at break are 1.0, 1.2, and 1.7 MPa for IPNs containing 25, 50, and 75 wt % PEGDM, respectively (Figure 8a). For PEO single networks, the stress at break increases, i.e., 0.3, 0.5, and 1.4 MPa for PEO networks containing 25, 50, and 75 wt % PEGDM, respectively (Figure 8b).

dx.doi.org/10.1021/ma201662h |*Macromolecules* 2011, 44, 9683–9691

As shown in Figure 9, the presence of the NBR network improves the IPN thermal stability in contrast to the PEO single network. For instance, the degradation temperature of NBR/PEO(50% PEGDM) IPN, in air, after 5% loss ($T_{d5\%}$), is close to 300 °C, 55 °C higher than the PEO network (Figure 9). Similar trends were also obtained for other PEO network compositions.

At this stage of the study, we can conclude that the presence of the NBR network strengthens the PEO mechanical and thermal properties. The IPN-based SPE is soft, flexible, and mechanically resistant. Furthermore, as observed by DSC (results not shown), the absence of the PEO crystalline phase should help to enhance its ionic conductivity.

3.6. Ionic Conductivity Studies. First, the ionic conductivity of IPNs and single networks were studied using LiTFSI as the electrolyte. The loading of the IPN, NBR, and PEO single networks with LiTFSI was achieved by means of a swelling process using propylene carbonate (PC) or water as solvent (1 mol L^{-1} LiTFSI) for 48 h. In this study, only networks and IPNs with 50% PEGDM were compared. After solvent evaporation (1 week under vacuum at 70 °C) the salt content was determined by a gravimetric technique, and ionic conductivity measures were carried out on dry samples (Table 3). It is noteworthy that the LiTFSI content in the NBR/PEO IPN swollen in PC was not the average value between NBR and PEO single networks as it is when materials are swollen with water. This could be due to the fact that the swelling ratio of PEO in the IPN by PC is significantly larger than that of the single PEO network in PC since it facilitates the incorporation of a higher content of LiTFSI in the PEO phase (Table 3). Figure 10 shows the temperature dependence of the ionic conductivity for LiTFSI loaded samples using PC as solvent. For all samples, this conductivity increases with temperature which can easily be explained by an increase in the mobility of charge carriers and the mobility of the polymer chain. Thus, the ionic conductivity of the NBR single network is close to 10^{-6} S cm^{-1} at 50 °C, corresponding to the value reported for linear NBR (un-cross-linked) by Ohno et al.[12] In the case of PEO(50% PEGDM) single network, the ionic conductivity at 50 °C is close to 2×10^{-5} S cm^{-1}. This value is slightly lower than the ionic conductivity of PEO networks synthesized by Watanabe et al.[35] from hyperbranched macromonomers (10^{-4} S cm^{-1} at 50 °C). The ionic conductivity behavior of the IPN is in between that of the two single networks (4.2×10^{-6} S cm^{-1} at 50 °C). As a result, NBR/PEO(50% PEGDM) IPN ionic conductivity increases from 2×10^{-7} to reach 2×10^{-5} S cm^{-1} when the temperature increases from 20 to 80 °C.

As PC swells both the NBR and PEO phases, Li^+ and $TFSI^-$ can migrate through both domains. Ionic conductivity of the NBR/PEO(50% PEGDM) IPN loaded with LiTFSI was also studied using water as solvent (1 mol L^{-1} LiTFSI, 48 h). Contrary to PC, water hardly swells the NBR phase (Table 3); therefore, only PEO regions facilitate the migration of ionic species. It is interesting to note in Figure 11 that the ionic conductivity is the same in both cases. In addition, the $[Li^+]/[-CH_2-CH_2-O-]$ ratio is similar

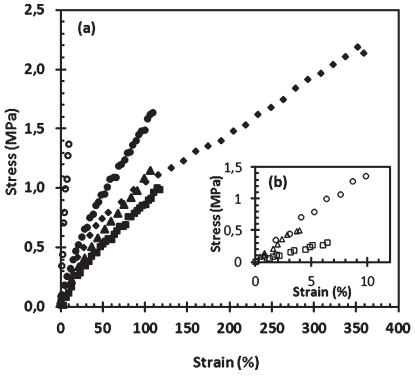

Figure 8. (A) Stress versus strain for NBR (◆) and PEO(75% PEGDM) (○) single networks and NBR/PEO IPNs with 25% PEGDM (■), 50% PEGDM (▲), and 75% PEGDM (●). (B) Stress versus strain for PEO(25% PEGDM) (□), PEO(50% PEGDM) (△), and PEO(75% PEGDM) (○) single networks.

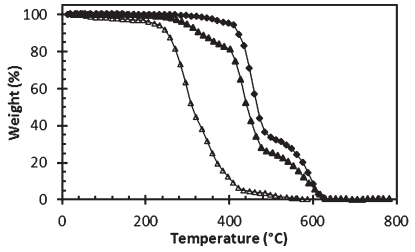

Figure 9. Weight versus temperature for PEO(50% PEGDM) (△) and NBR (◆) single networks and NBR/PEO(50% PEGDM) IPN (▲).

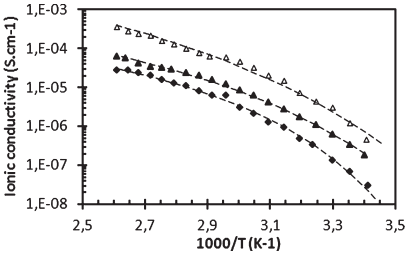

Figure 10. Ionic conductivity versus temperature for NBR (◆), for PEO(50% PEGDM) (△) single networks, and for NBR/PEO(50% PEGDM) IPN (▲) loaded with LiTFSI in PC. Dashed lines: calculation according to the VTF equation.

Table 3. LiTFSI Content and Ionic Conductivity with LiTFSI Loaded with PC; LiTFSI Content and $[Li^+]/[-CH_2-CH_2-O-]$ Ratio for LiTFSI Loaded with H_2O

samples	swelling ratio in PC (wt %)	LiTFSI content (wt %) loaded with PC	ionic conductivity (S cm^{-1}) at 50 °C (LiTFSI loaded with PC)	LiTFSI content (wt %) loaded with H_2O	[Li]/[EO] (LiTFSI) (loaded with H_2O)
NBR	258	57	1.3×10^{-6}	2	
PEO(50% PEGDM)	131	55	2.0×10^{-5}	66	0.13 (~1/7.7)
NBR/PEO(50% PEGDM)	236	78	4.2×10^{-6}	33.5	0.14 (~1/7.1)

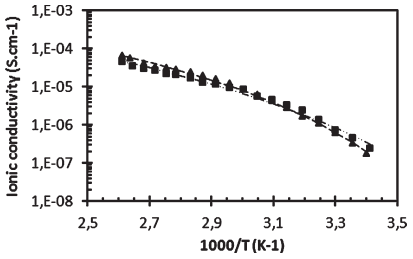

Figure 11. Ionic conductivity versus temperature for NBR/PEO(50% PEGDM) IPN loaded with LiTFSI in PC (▲) or in water (■). Dashed lines: calculation according to the VTF equation.

Table 4. VTF Parameters of Single Networks and IPNs after Loading with LiTFSI

	A (S cm^{-1} K$^{1/2}$)	B (K)	T_0 (K)	LiTFSI load[a] (%)
PEO(50% PEGDM)	4.374	1124	206	55 (PC)
NBR	0.036	574	243	57 (PC)
NBR/PEO(50% PEGDM) IPN	0.177	803	220	78 (PC)
NBR/PEO(50% PEGDM) IPN	0.224	1030	196	33.5 (H_2O)

[a] Solvent used for the introduction of LiTFSI into the network is given in parentheses.

in the two cases—PEO single network and corresponding IPN—confirming the hypothesis that water only swells the PEO phase, to the exclusion of the IPN NBR phase. In view of these results, we can state that the entire PEO phase of NBR/PEO(50% PEGDM) IPN is accessible to the LiTFSI,[36] and the ionic conductivity of the IPN is ensured by the PEO phase. In addition to TEM observations of NBR/PEO IPNs, these results imply that the PEO network is continuous (or nearly so) within the material. Since the NBR network is formed first; the NBR/PEO IPN exhibits a cocontinuity of domains.

In general, the temperature dependence of the ionic conductivity has been described as exhibiting two possible behaviors. The first is characterized by an Arrhenius relation (see eq 6):

$$\sigma(T) = A \exp(-E_a/RT) \quad (6)$$

Arrhenius behavior is usually observed when the ionic conductivity is decoupled from the polymer chain dynamics. In the second behavior, the data are fitted to the Vogel−Tamman−Fulcher (VTF) empirical model (eq 7):[37]

$$\sigma(T) = AT^{-1/2} \exp[-B/(T - T_0)] \quad (7)$$

where A and B are constants related to the number of charge carriers and the ion conduction activation energy, respectively. T_0 is considered as the idealized temperature corresponding to zero configuration entropy, according to Adam−Gibbs analysis. T_0 is usually 30−50 K lower than the material's glass transition temperature obtained by DSC. VTF behavior is observed when the ionic mobility is coupled with the polymer chain movements, characterized by a curvature in the temperature/ionic conductivity plot. In our case, as can be seen in Figures 10 and 11, all samples exhibit VTF behavior, illustrating an interaction between dissociated ions and the polymer network. Table 4 summarizes the fitting parameters of the VTF function as well as the LiTFSI load of each system. T_0 was fixed at 50 K below the system's T_g. All fitting was achieved using an acceptable correlation coefficient ($R^2 > 0.99$).

The VTF parameters of PEO(50% PEGDM) single network loaded with LiTFSI are in the same order of magnitude as with the linear PEO−LiTFSI system with a [Li]/[EO] ratio between 0.1 and 0.33, reported by Flojanczyk et al.[38] It is interesting to note that the PEO A value is 100 times higher than that of NBR even though their LiTFSI loads are similar. Since the A value is related to the quantity of charge carriers and is consistent with expectations for dissociated electrolytes,[37] it is reasonable to suggest that LiTFSI is more dissociated in PEO network than in an NBR one. This assertion is additionally supported by the complexation between Li^+ and PEO in solid state, as is widely reported. The A values of IPNs is between those of parent networks. Despite a lower LiTFSI loading content when using H_2O as solvent to introduce the salt, little difference is observed in the A value of the IPNs loaded with LiTFSI. This seems to indicate that the effective quantity of charge carriers available for conduction is governed by salt dissociated from the PEO phase as suggested above.

On the other hand, the highest B values were observed in PEO(50% PEGDM) single network and NBR/PEO IPN loaded with LiTFSI/water, where the salts are introduced exclusively in the PEO phase. Since the B value reflects the temperature dependence of the conductivity, the high B value confirms the interaction of Li^+ ions with ethylene oxide units in the PEO phase. The lowest B value is observed in the NBR single network since minimal interaction occurs between NBR and ionic species. In the case of NBR/PEO IPN loaded with LiTFSI/PC, an intermediate B value is observed since the salt is present in both the NBR and PEO phases. It can be deduced that the mobility of the ionic species in the PEO phase is more temperature dependent, and their dissociation is better than in the NBR phase due to the complexation of Li^+ ions.

The study of IPNs with LiTFSI as electrolyte demonstrates a cocontinuous structure of IPN providing the highest ionic conductivity of 4.2×10^{-6} S cm^{-1} at 50 °C. Higher ionic conductivity could be obtained by using ionic liquids as an electrolyte.[39,40] Among them, EMITFSI is one of the best candidates due to its high ionic conductivity, nonvolatility, and its low viscosity.[41] In addition, EMITFSI has a high affinity to polymers with polar groups which made it compatible for both the NBR[11,18] and PEO phases of IPN. The weight proportion of EMITFSI loaded into the networks can be controlled by the swelling time in neat EMITFSI. The maximum EMITFSI uptake was reached, for all studied samples, within 1 week. Table 5 shows the maximum uptake of EMITFSI loading in single networks and IPNs. The ionic liquid uptake in NBR is 85 wt % and can reach 180 wt % in a PEO single network (PEO(25% PEGDM)). This supports the higher affinity of EMITFSI to PEO network compared with the NBR network. In addition, the synergistic effect of IPNs is also observed in that the ionic liquid uptake is higher in IPNs than in either PEO or NBR single networks. On the other hand, the EMITFSI uptake increases with the decrease of cross-linking density of PEO networks, whether in single network or in IPNs. Thus, the EMITFSI uptake drops from 180 to 100 wt % and from 260 to 150 wt % while the PEGDM proportion decreases from 75% to 25% in PEO single networks and IPNs, respectively.

Figure 12 shows the temperature dependence of the ionic conductivity of the EMITFSI-swollen PEO and NBR single networks. It demonstrates that the PEO partner is 20−100 times

Table 5. EMITFSI Uptake (wt %) of Networks and IPNs after 1 week Swelling in Neat EMITFSI

samples	EMITFSI uptake (wt %)	ionic conductivity at 30 °C (S cm^{-1})
NBR	85	1.7×10^{-5}
PEO(25% PEGDM)	180	1.7×10^{-3}
PEO(50% PEGDM)	140	9.3×10^{-4}
PEO(75% PEGDM)	100	4.5×10^{-4}
NBR/PEO(25% PEGDM)	260	6.7×10^{-4}
NBR/PEO(50% PEGDM)	200	6.7×10^{-4}
NBR/PEO(75% PEGDM)	150	2.9×10^{-4}

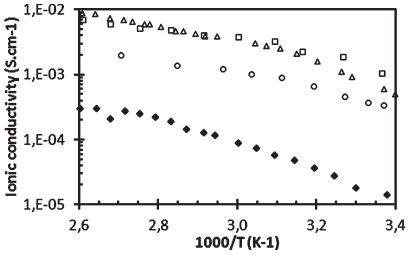

Figure 12. Ionic conductivity for NBR (◆), PEO(25% PEGDM) (□), PEO(50% PEGDM) (△), and PEO(75% PEGDM) (○) single networks loaded with EMITFSI.

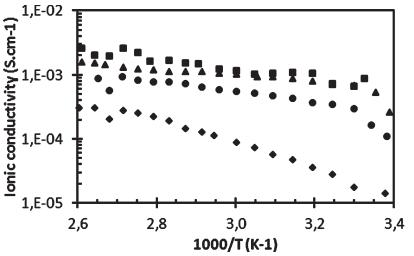

Figure 13. Ionic conductivity for NBR single network (◆) and NBR/PEO IPNs with 25% PEGDM (■), 50% PEGDM (▲), and 75% PEGDM (●) loaded with EMITFSI.

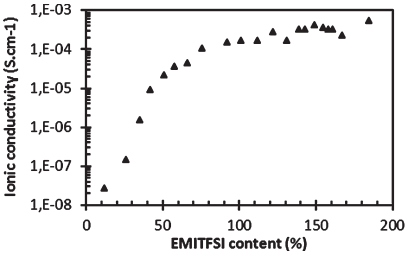

Figure 14. NBR/PEO(50% PEGDM) IPN ionic conductivity for different EMITFSI contents in weight (at 25 °C).

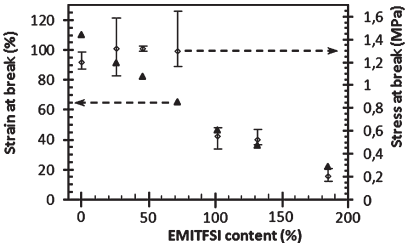

Figure 15. Strain (▲) and stress (◇) at break versus EMITFSI content (in wt %) for NBR/PEO(50% PEGDM) IPN (at 25 °C).

more conductive than the NBR one. Moreover, the ionic conductivity of the PEO network increases with increasing EMITFSI uptake since the electrolyte content increases. The cross-linking density of PEO networks plays an important role in ionic conductivity. The conductivity of PEO networks containing 25 and 50 wt % PEGDM reaches a very high value, i.e., 10^{-3} S cm^{-1} at 30 °C up to 5×10^{-3} S cm^{-1} at 80 °C. These conductivities are only 1 order of magnitude lower than that of neat EMITFSI (8×10^{-3} S cm^{-1} at 25 °C[41]). However, an increase in PEGDM content up to 75 wt % leads to a decrease in ionic conductivity by a factor of 3 in the 30−80 °C temperature range. Indeed, ionic conductivity can be improved by introducing short poly(ether oxide) side chains into the PEO networks as chain ends in order to build a "branched" PEO network.[42] With more flexible chains, the free volume available for the ionic mobility would be much higher than in unbranched or low-branched networks. Therefore, PEO networks containing 25 and 50 wt % of PEGDM exhibit the highest ionic conductivity as already demonstrated.[43]

For EMITFSI-swollen IPNs (Figure 13), conductivity values are slightly lower than that of PEO single networks. As in PEO single network, the IPN ionic conductivity decreases with the increase of PEGDM content. At room temperature, IPNs and PEO single networks have similar ionic conductivity (close to 0.7×10^{-3} S cm^{-1} at 30 °C). Therefore, the presence of the PEO network within the NBR network leads to a material having good ionic conductivity at room temperature.

It is also interesting to study the ionic conductivity and elongation at break of the NBR/PEO(50% PEGDM) IPN as a function of EMITFSI content. Indeed, the addition of ionic liquid and liquid electrolyte generally increases the ionic conductivity but tends to weaken polymer membranes. In some cases, gel-SPEs, swollen with liquid electrolytes, are very brittle and can be destroyed during handling.[44] For NBR/PEO(50% PEGDM) IPN, the ionic conductivity at 25 °C increases with the EMITFSI ratio and reaches a plateau at approximately 2.6×10^{-4} S cm^{-1} when EMITFSI content exceeds 75% (Figure 14).

In parallel, the IPN elongation at break decreases with increasing EMITFSI content (Figure 15). It occurs at 110% strain without ionic liquid but drops to 20% when the network is swollen to saturation. However, for an EMITFSI swelling of less than 75%, the stress at break remains close to 1.3 MPa. It then decreases rapidly to 0.2 MPa for 185% EMITFSI (saturation) (Figure 15). Presumably below 75% EMITFSI swelling, most of the IPN chains are not stretched to the maximum, and the force required to break the material remains the same as for dry film. For higher swelling degrees, most of the chains are stretched and the film breaks when subjected to minimal stress. It is interesting to note that the PEO(50% PEGDM) single network in the presence of ionic liquid is too weak to undergo the tensile test. Thus, the NBR/PEO(50% PEGDM) IPN swollen with 75% of EMITFSI leads to a material possessing a good ionic conductivity at room temperature (10^{-4} S cm^{-1}) while maintaining the necessary mechanical properties required for a solid polymer electrolyte (elongation at break of 65% for a stress of 1.3 MPa).

4. CONCLUSION

A series of solid polymer electrolytes based on NBR/PEO interpenetrating polymer networks containing 25, 50, and 75 wt % PEGDM in the PEO network were synthesized. The IPNs were developed using a two-step process where the PEO network is formed within the NBR network.

This study reveals that the NBR network presence improves the mechanical properties of PEO single network; i.e., elongation at break is 10−20 times higher for NBR/PEO IPNs than that observed with PEO single networks. Moreover, NBR/PEO IPNs with 25 and 50 wt % PEGDM, swollen by EMITFSI at saturation, exhibit ionic conductivity value (at room temperature) comparable to that of PEO single networks with the same PEGDM content.

In the dry state, NBR/PEO(50% PEGDM) IPN is the best compromise with good mechanical properties and an elongation at break of 110% for a stress of 1.2 MPa. Swollen with 75% of EMITFSI, this IPN leads to a material whose ionic conductivity is higher than 10^{-4} S cm^{-1} at room temperature, while maintaining an elongation at break of 65% for a stress of 1.3 MPa. At the maximum uptake of EMITFSI, NBR/PEO(50% PEGDM) IPN has an ionic conductivity close to 10^{-3} S cm^{-1} at 30 °C. These values are very promising and demonstrate their suitability for use as base materials in actuators and self-supporting electrochromic devices.

AUTHOR INFORMATION

Corresponding Author

*E-mail: Frederic.vidal@u-cergy.fr.

ACKNOWLEDGMENT

This work has been supported by Délégation Générale de l'Armement. The authors acknowledge Serge Fanget from Lanxess Emulsion Rubber for graciously proving NBR and Isabelle Anselme-Bertrand from the Centre de Microscopie Electronique Stéphanois (CMES) for TEM measurements.

REFERENCES

(1) Wright, P. V. *Br. Polym. J.* **1975**, *7*, 319.
(2) Armand, M.; Chabago, J. M.; Duclot, M. *The 2nd International Conference on Solid Electrolytes*; St. Andrews: Scotland, 1978.
(3) Macallum, J. R. *Polymer Electrolyte Reviews 1 and 2*; Vincent, C. A., Ed.; Elsevier: London, 1987−1989.
(4) Gray, F. M. *Solid Polymer Electrolytes*; VCH: New York, 1991.
(5) Fenton, D. E.; Parker, J. M.; Wright, P. V. *Polymer* **1973**, *14*, 589.
(6) Armand, M. *Solid State Ionics* **1983**, *9*−*10*, 745.
(7) Valléea, A.; Besnera, S.; Prud'Homme, J. *Electrochim. Acta* **1992**, *37*, 1579.
(8) Chintapalli, S.; Frech, R. *Solid State Ionics* **1996**, *86*−*88*, 341.
(9) Aihara, Y.; Arai, S.; Hayamizu, K. *Electrochim. Acta* **2000**, *45*, 1321.
(10) Ichino, T.; Matsumoto, M.; Takeshita, Y.; Rutt, J. S.; Nishi, S. *Electrochim. Acta* **1995**, *40*, 2265.
(11) Marwanta, E.; Mizumo, T.; Nakamura, N.; Ohno, H. *Polymer* **2005**, *46*, 3795.
(12) Marwanta, E.; Mizumo, T.; Ohno, H. *Solid State Ionics* **2007**, *178*, 227.
(13) Nakajima, H.; Ohno, H. *Polymer* **2005**, 11499.
(14) Kang, Y.; Kim, H. J.; Oh, B.; Cho, J. H. *J. Power Sources* **2001**, *92*, 255.
(15) Zhang, Z.; Fang, S. *Electrochim. Acta* **2000**, *45*, 2131.
(16) Grosz, M.; Boileau, S.; Guégan, P.; Chéradame, H.; Deshayes, A. *Polym. Prepr. (Am. Chem. Soc., Div. Polym. Chem.)* **1997**, *38*, 612.
(17) Matoba, Y.; Ikedab, Y.; Kohjiya, S. *Solid State Ionics* **2002**, *147*, 403.
(18) Cho, M.; Seo, H.; Nam, J.; Choi, H.; Koo, J.; Lee, Y. *Sens. Actuators, B* **2007**, *128*, 70.
(19) Li, J.; Pratt, L. M.; Khan, I. M. *J. Polym. Sci., Part A: Polym. Chem.* **1995**, *33*, 1657.
(20) Acosta, J. L.; Enrique, M. *J. Appl. Polym. Sci.* **1996**, *60*, 1185.
(21) Munichandraiah, N.; Sivasankar, G.; Scanlon, L. G.; Marsh, R. A. *J. Appl. Polym. Sci.* **1997**, *65*, 2191.
(22) Watanabe, M.; Sanu, K.; Ogata, N.; Kobayashi, T.; Ohtaki, Z. *J. Appl. Phys.* **1985**, *57*, 123.
(23) Florjanczyk, Z.; Krawiec, W.; Wieczorek, W.; Siekierski, M. *J. Polym. Sci., Part B: Polym. Phys.* **1995**, *33*, 629.
(24) Allcock, H. R.; O'Connor, S. J. M.; Olmeijer, D. L.; Napierala, M. E.; Cameron, C. G. *Macromolecules* **1996**, *29*, 7544.
(25) Alloin, F.; Herrero, C. R.; Sanchez, J. Y.; Delabouglisem, D.; Armand, M. *Electrochim. Acta* **1995**, *40*, 1907.
(26) Zhang, Z.; Fang, S. *J. Appl. Polym. Sci.* **2000**, *77*, 2957.
(27) Ichikawa, K.; Dickinson, L. C.; MacKnight, W. J.; Watanabe, M.; Ogata, N. *Polymer* **1992**, *33*, 4699.
(28) Basak, P.; Manorama, S. V. *Solid State Ionics* **2004**, *167*, 113.
(29) Hou, X.; Siow, K. S. *Polymer* **2000**, *41*, 8689.
(30) Klempner, D., Sperling, L. H., Utracki, L. A., Eds.; *Interpenetrating Polymer Networks*; Adv. Chem. Ser. 239; American Chemical Society: Washington, DC, 1994.
(31) Vidal, F.; Plesse, C.; Aubert, P.-H.; Beouch, L.; Tran-Van, F.; Palaprat, G.; Verge, P.; Yammine, P.; Citerin, J.; Kheddar, A.; Sauques, L.; Chevrot, C.; Teyssie, D. *Polym. Int.* **2010**, *59*, 313.
(32) Plesse, C.; Vidal, F.; Gauthier, C.; Pelletier, J.-M.; Chevrot, C.; Teyssié, D. *Polymer* **2007**, *48*, 696.
(33) Akiba, M.; Hashim, A. S. *Prog. Polym. Sci.* **1997**, *22*, 475.
(34) Valentin, J. L.; Rodriguez, A.; Marcos-Fernandez, A.; Gonzalez, L. *J. Appl. Polym. Sci.* **2005**, *96*, 1.
(35) Watanabe, M.; Hirakimoto, T.; Mutoh, S.; Nishimoto, A. *Solid State Ionics* **2002**, *148*, 399.
(36) Gauthier, C.; Plesse, C.; Vidal, F.; Pelletier, J.-M.; Chevrot, C.; Teyssié, D. *Polymer* **2007**, *48*, 7476.
(37) Xu, W.; Sun, X.-G.; Austen Angell, C. *Electrochim. Acta* **2003**, *48*, 2255.
(38) Flojanczyk, Z.; Zygadao-Monikowska, E.; Affek, A.; Tomaszewska, A.; Lasinska, A.; Marzantowicz, M.; Dygas, J. R.; Krokb, F. *Solid State Ionics* **2005**, *176*, 2123.
(39) Vidal, F.; Plesse, C.; Palaprat, G.; Juger, J.; Citerin, J.; Kheddar, A.; Chevrot, C.; Teyssié, D. *Adv. Sci. Technol.* **2008**, *61*, 8.
(40) Plesse, C.; Vidal, F.; Randriamahazaka, H.; Teyssié, D.; Chevrot, C. *Polymer* **2005**, *46*, 7771.
(41) Bonhôte, P.; Dias, A.-P.; Papageorgious, N.; Kalyanasundaram, K.; Grätzel, M. *Inorg. Chem.* **1996**, *35*, 1168.
(42) Nishimoto, A.; Agehara, K.; Furuya, N.; Watanabe, T.; Watanabe, M. *Macromolecules* **1999**, *32*, 1541.
(43) Verge, P.; Mallouki, M.; Beouch, L.; Aubert, P.-H.; Vidal, F.; Tran-Van, F.; Teyssié, D.; Chevrot, C. *Mol. Cryst. Liq. Cryst.* **2010**, *521*, 353.
(44) Shaplov, A.; Goujon, L.; Vidal, F.; Lozinskaya, E. I.; Meyer, F.; Ma lyshkina, I. A.; Chevrot, C.; Teyssié, D.; Odinets, I. L.; Vygodskii, Y. S. *J. Polym. Sci., Part A: Polym. Chem.* **2009**, *47*, 4245.